Experimental and Numerical Investigation of the Influence of Cutting Speed and Feed Rate on Forces in Turning of Steel

János KUNDRÁK[1,a *], Gergely SZABÓ[1,b] and Angelos P. MARKOPOULOS[2,c]

[1]University of Miskolc, Institute of Manufacturing Science, Miskolc, Hungary, Miskolc-Egyetemváros H-3515, Hungary

[2]National Technical University of Athens, School of Mechanical Engineering, Section of Manufacturing Technology, Heroon Politechniou 9, 15780, Athens, Greece

[a]kundrak@uni-miskolc.hu, [b]gergely.szabo@uni-miskolc.hu, [c]amark@mail.ntua.gr

Keywords: Cutting forces, experimental investigation, numerical modeling, finite element simulation.

Abstract. The impact of cutting speeds and feed rates on the components of the forces exerted on a 16MnCr5 steel workpiece is experimentally measured, when turning with PCBN tool. The cutting speed range of the tests varies between 90 to 240 m/min while the feed rate is between 0.05 and 0.25 mm/rev for each cutting speed, allowing for the determination of the influence of cutting conditions on forces. Additionally, finite elements models for the simulation of the aforementioned experiments are provided. The proposed models exhibit good correlation of their results on cutting forces and chip formation with the measurements and observations of the experiments. Furthermore, the models can provide a wide range of additional parameters, i.e. plastic strain rates and temperatures within the workpiece. Results of the presented analysis can be used for an efficient process planning for the turning of steels under cutting conditions used in the industry.

Introduction

Machining of hardened steels, for roughing and most importantly for finishing, is of great importance for the industry. Today's demand for higher productivity, quality and surface integrity of components manufactured by machining has led to the extensive use of cubic boron nitride (CBN) and polycrystalline cubic boron nitride (PCBN) tools. Since it was first introduced as a cutting tool material, PCBN has evolved to become a common machining solution for the processing of difficult-to-machine materials, especially for high cutting speed values. PCBN tools retain their properties at elevated cutting temperatures, without compromising the overall quality of the workpiece. Machining with these tools has proven to be an equal or even better alternative to rival conventional and unconventional finishing processes, in terms of the characteristics of the surface and the subsurface of the finished part, which greatly affect its life cycle [1-3].

One of the most important features of the cutting process is chip formation; various types of chip can be produced. According to Ernst's classification, three chip types may be identified, namely discontinuous, continuous and continuous with built-up edge [4]. However, at high speeds, a fourth type is observed, the serrated or segmented chip as is usually found in the relevant literature [5-7]. Although it is generally accepted that chip segmentation is energetically favorable, tool wear issues exist [8]. This saw-toothed chip is responsible for excessive chip-tool friction and temperatures at the rake face of the tool that consequently provoke significant wear and tool life reduction [9]. In turning of hard materials with PCBN tools, negative rake angle is commonly applied, which creates high compressive stresses both on the cutting edge and the workpiece. Because of the brittle nature of the workpiece material, high compressive stresses form a crack instead of a material flow. As a result, the material in front of the tool parts from the chip root as a segment. The crack releases the stored energy and thus acts as a sliding surface for the material segment, allowing it to be forced out between the parting surfaces. Concurrently, heating of the material due to plastic deformation and friction takes place at the cutting tool leading edge and the heat supplied changes the behaviour of

the material, which is not completed parted; thus a continuous chip is formed. Once the chip segment has slid away, the cutting pressure results in the formation of a new crack and chip segment. The individual chip segments are linked by the small proportion of the material, which is plastically deformed and heated to a high temperature. This characteristic chip formation process influences the residual stress state of the machined surface. This factor is of particular interest as it decisively determines component behaviour. Additionally, other investigators observe increase in the friction force and tool wear, at high speeds, after the transition from continuous chip to serrated chip, especially for hard ferrous materials [10, 11]. However, tool life can be prolonged by optimizing cutting parameters, cutting conditions and machining strategy [12].

Chip formation mechanism determines cutting forces in machining. Furthermore, cutting speed, feed rate and depth of cut are the main controlling parameters in metal cutting; a close relation between the cutting conditions and cutting forces may be identified. In this paper, the effect of cutting speed and feed rate on the three components of the cutting force is investigated experimentally and the results of the investigation are discussed. Moreover, Finite Element Method (FEM) models are constructed that can reliably predict the outcome of the process, in relation to cutting forces and chip formation. The advantages of the proposed FEM models are that they are simple in implementation and can provide extra information of the conditions within the cutting zone, e.g. temperatures of the workpiece and the chip, which would be difficult to obtain otherwise.

Materials and Methods

Experimental work

For the investigation of the influence of the cutting speed and feed rate on the cutting forces in turning of hard steels with PCBN tools, several experiments were performed. Workpieces of 16MnCr5 steel were cut. In table 1, the tool insert features are summarized.

Table 1: Tool insert features

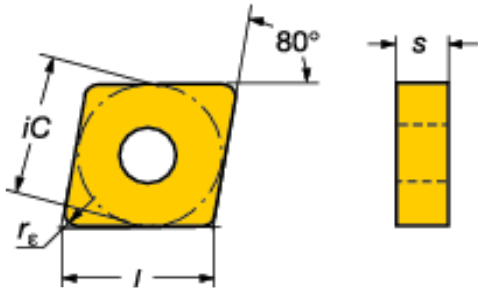

Type of insert	CNGA120408S01030A 7015
Manufacturer	SANDVIK COROMANT
Material	PCBN
Tool edge	Normal
iC	12.7 mm
r_ε	0.8 mm
s	4.76 mm
l	12 mm

For the experiments, five cutting speeds, namely 90, 120, 150, 180 and 240 m/min, and five feed rates, namely 0.05, 0.10, 0.15, 0.20 and 0.25 mm/rev were tested. In all the experiments the depth of cut was constant and equal to 0.1 mm. The three force components were measured by a Kistler 9257 dynamometer. The data from the measuring device were collected as graphs, as well as raw data and were stored in a PC for further processing.

FEM simulation

The models presented in this paper were prepared with Third Wave AdvantEdge software, which is solely dedicated for machining simulation. Third Wave AdvantEdge software is a widely used commercial FEM program, employed both in the academia and the industry; it provides validated, detailed information about heat flow, temperatures, stresses, tool life, and surface characteristics for machining processes. The program menus are designed in such a way that allow the user to minimize model preparation time. Furthermore, it possesses a wide database of workpiece and tool materials commonly used in cutting operations, offering all the required data for effective material modeling. AdvantEdge is a Lagrangian, explicit, dynamic code which can perform coupled thermo-

mechanical transient analysis. The program applies adaptive meshing and continuous re-meshing for chip and workpiece, allowing for accurate results.

For the investigation presented in this paper, the 2D version of Third Wave AdvantEdge^{TM} ver. 5.3 was employed and orthogonal cutting models were investigated. One of the most important features of this commercial software is the ability to choose a suitable material model. Material modelling pertains to the flow characteristics of the workpiece material and the corresponding equations to be included in the FEM model. These constitutive equations describe the flow stress or instantaneous yield strength at which work material starts to plastically deform or flow. The proposed models are built with the material following the Johnson-Cook model [13]. The equation consists of three terms the first one being the elasto-plastic term to represent strain hardening, the second is viscosity, which demonstrates that material flow stress increases for high strain rates and the temperature softening term; it is a thermo-elasto-visco-plastic material constitutive model, described as [14]:

$$\sigma_{red} = \left(A + B \cdot e^{n}\right) \cdot \left(1 + C \ln\left(\frac{\dot{\varepsilon}}{\varepsilon_0}\right)\right) \cdot \left(1 - \left(\frac{T - T_{room}}{T_m - T_{room}}\right)\right)^{m} \quad (1)$$

where σ_{red} is the reduced stress, ε is the plastic strain, $\dot{\varepsilon}$ is the plastic strain rate, $\dot{\varepsilon}_0$ is the reference plastic strain rate, T is the workpiece temperature, T_m is the workpiece melting temperature, T_{room} is the room temperature, coefficient A is the yield strength, B is the hardening modulus, C is the strain rate sensitivity coefficient, n is the hardening coefficient, and m is the thermal softening coefficient. The aforementioned parameters can either be determined by material tests or predicted and are widely used for the simulation of metal cutting [15-18]. The Johnson-Cook parameters used in the presented analysis are shown in Table 2 [19].

Table 2: Johnson-Cook parameters for 16MnCr5 steel

σ_{red} [MPa]	A [MPa]	B [MPa]	C [-]	n [-]	m [-]
400	588	680	0.057	0.4	0.7

Results and discussion

Two experimental force measurements were taken for each combination of the cutting conditions. In Table 3 the experimental results with the average force of the two measurements are tabulated. Passive force F_p is the highest of the three components, as expected. In the same table, the ratio of the passive force F_p to the cutting force F_c is also shown. Furthermore, for the F_p/F_c ratio, results are categorized, by their value, to regions, indicated by different shade of grey in the table.

Based on the data included in Table 3, the graph of Fig. 1 is constructed. It contains the cutting force F_c contours at various intervals, for all the tested cutting conditions. Fig. 2 and Fig. 3 depict similar graphs for passive force F_p and the ratio F_p/F_c, respectively.

From Table 3 and the corresponding graphs it can be said that some general trends in the variation of the force components can be identified. Forces increase for an increase in feed rate and decrease for an increase in cutting speed. This trend is not unusual and is reported for similar results [5]. The values of F_f, almost for every experimental conditions combination, lie in the interval between 20-40 N.

It is, however, interesting to notice in Fig. 3 that a peak is formed in the far left area of the graph. In this area, the F_p/F_c ratio is much higher than in the other parts of the graph. Indeed, in Table 3, for feed rates 0.10 to 0.25 mm/rev, the F_p/F_c ratio takes values between 2 and 4, while for feed rate of 0.05, F_p/F_c ratio is higher than 4; for cutting speed of 120 m/min it is higher than 18. An explanation for this can be given, based on the observation that the feed is comparable to the cutting tool edge radius. In this case, the cutting tool flank face creates a compressive plastic zone underneath it;

cutting force decreases and at the same time passive increases drastically, causing this irregular behavior.

Table 3. Measured cutting forces

	Feed rate	**Cutting speed** [m/min]				
	[mm/rev]	90	120	150	180	240
F_c [N]	0.05	12.4	3.6	8.8	7.0	19.7
	0.10	30.2	24.0	45.6	31.8	33.4
	0.15	47.1	46.9	61.1	62.0	47.9
	0.20	66.5	74.2	77.3	68.3	56.7
	0.25	87.1	86.7	75.7	66.2	50.9
F_p [N]	0.05	80.5	67.7	73.8	47.1	94.9
	0.10	104.0	86.5	111.5	107.0	118.5
	0.15	124.0	106.0	132.0	138.5	126.0
	0.20	141.0	142.5	150.5	134.0	118.0
	0.25	145.0	152.0	139.5	119.5	96.2
F_f [N]	0.05	23.7	21.6	22.1	46.7	28.9
	0.10	33.0	28.2	31.5	32.4	33.5
	0.15	35.3	31.4	35.5	40.3	33.1
	0.20	36.5	37.7	37.9	34.2	30.3
	0.25	35.2	36.2	32.7	29.9	22.8
F_p/F_c	0.05	6.48	18.84	8.42	6.77	4.82
	0.10	3.44	3.60	2.45	3.36	3.55
	0.15	2.64	2.26	2.16	2.23	2.63
	0.20	2.12	1.92	1.95	1.96	2.08
	0.25	1.66	1.75	1.84	1.81	1.89

0-2 2-4 4-6 6-8 8-10 >18

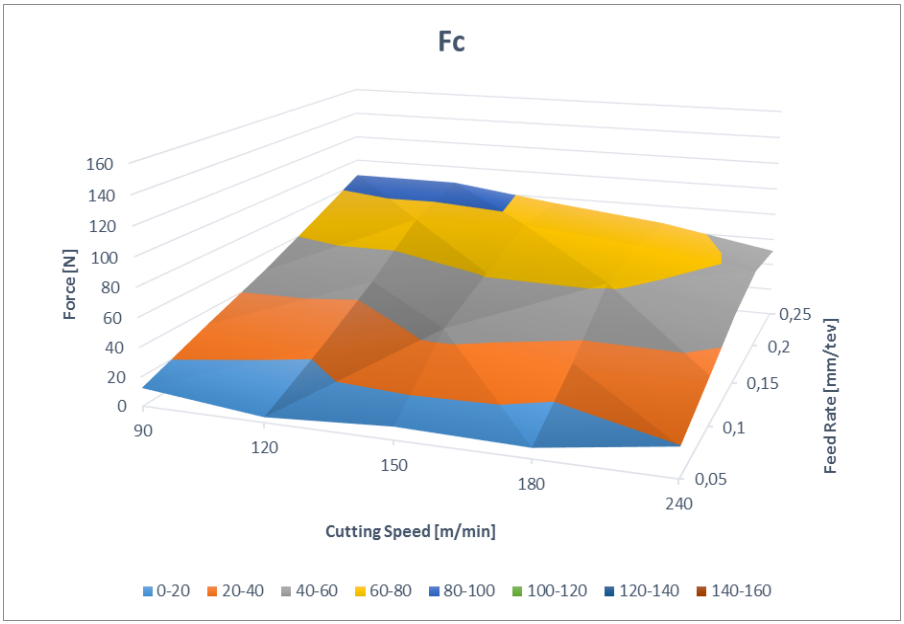

Figure 1: Cutting force F_c for various cutting conditions

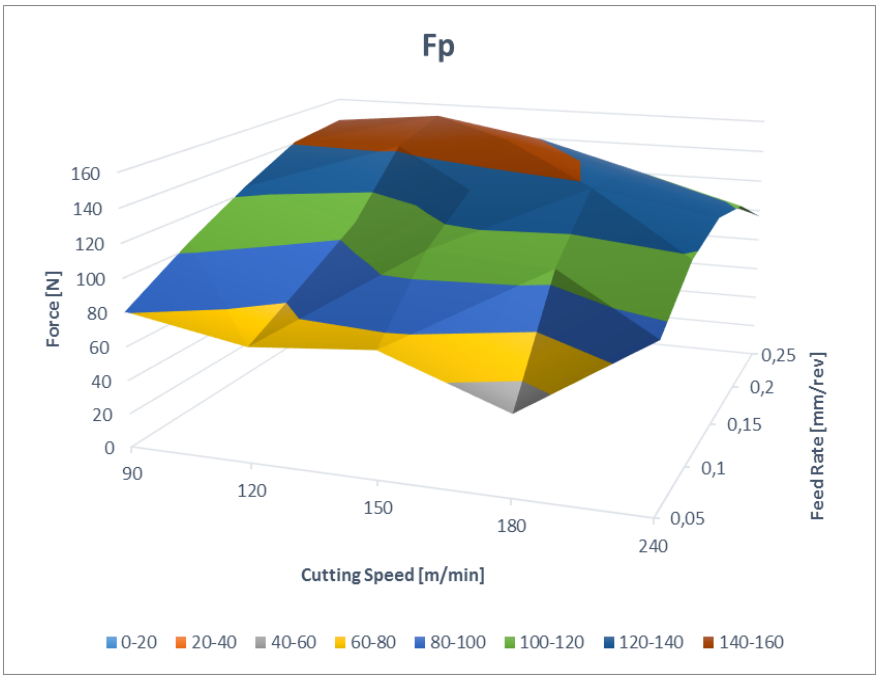

Figure 2: Passive force F_p for various cutting conditions

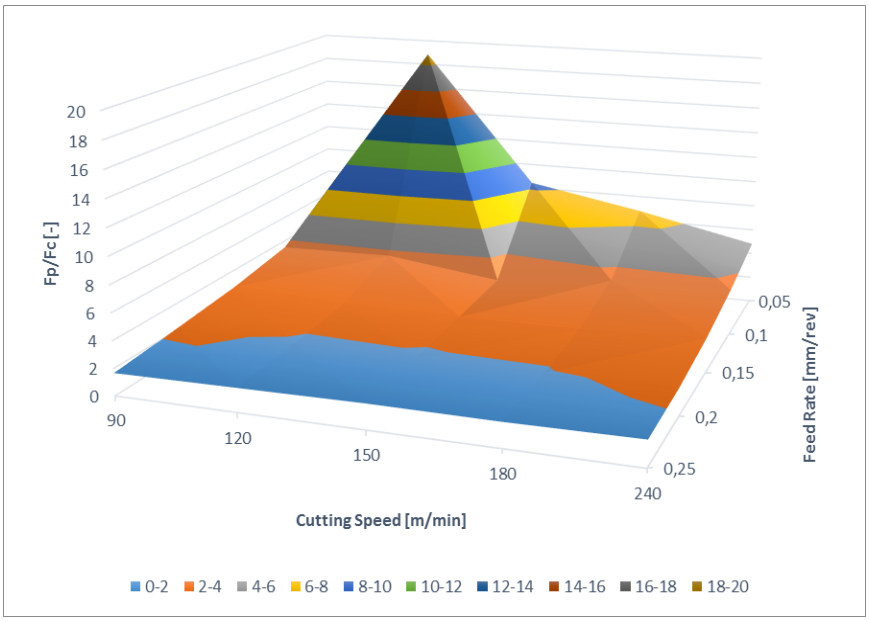

Figure 3: Ratio F_p/F_c for various cutting conditions

For the simulations presented in this paper, the cutting tool geometry was implemented in the FEM software, for accurate modeling of the process. The cutting conditions used in the experiments were also used as cutting conditions of the models. Indicatively, in Table 4 the numerical results for some of the proposed models are presented. The cutting forces are relatively well predicted; especially the F_p component. It is not unusual in machining simulation to underestimate either the cutting or the passive force component [20]. This is mainly attributed to the features of contact conditions modelling, for the high stresses, strain rates and temperatures encountered in machining.

However, results indicate that the models can predict well the chip formation mechanism presented in the turning of 16MnCr5 with PCBN tools at cutting speeds. The characteristic saw-toothed form of the chip is present in all simulations. It is worth noting the high strain rates of the shear zone and the chip, in all the simulated results.

Table 4: Numerical results for forces and plastic stain, for depth of cut 0.10 mm, feed rate 0.10 mm/rev and cutting speed a) 90 m/min, b) 120 m/min, c) 150 m/min, d) 180 m/min, e) 240 m/min

a	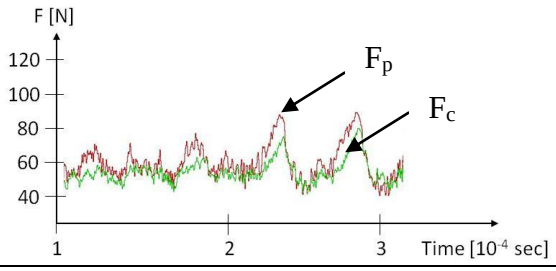	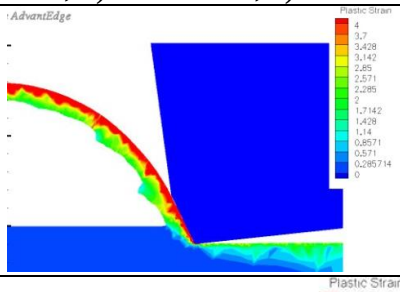
b	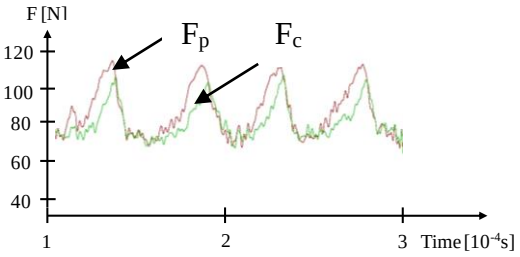	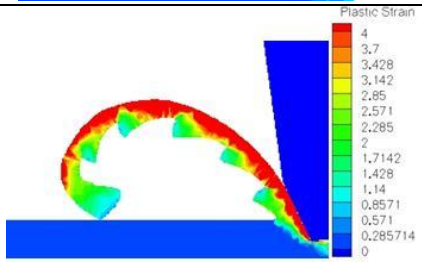
c	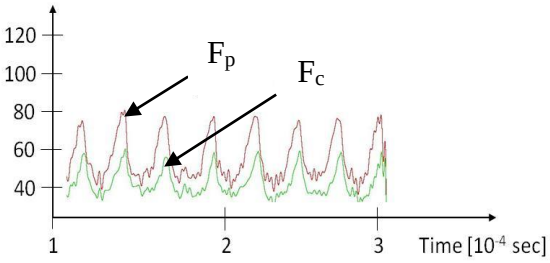	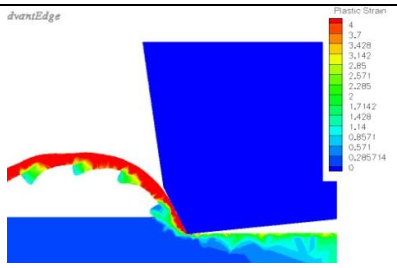
d	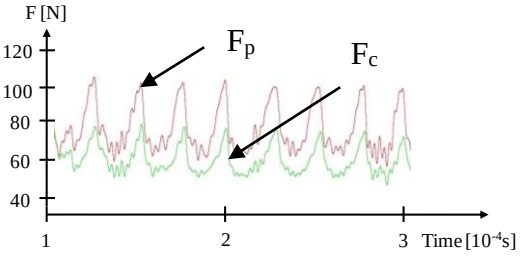	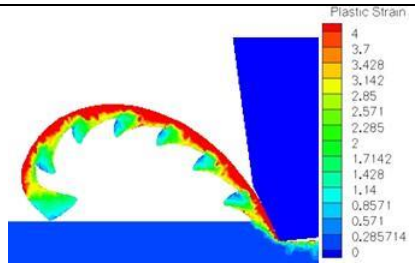
e	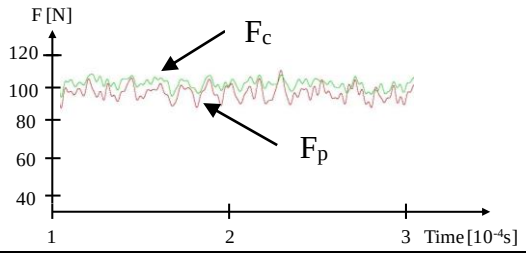	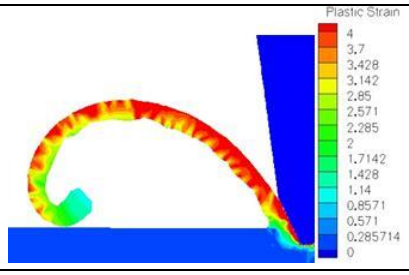

The models, except the prediction of cutting forces, can also be used for the prediction of the cutting temperatures that are difficult to be obtained experimentally. In Fig. 4(a) and Fig. 4(b), two simulation snapshots at the same time step, in the steady state condition of the simulation, are depicted with focus in the cutting zone. The former being for cutting speed equal to 90 m/min and feed rate of 0.10 mm/rev, while the latter being for cutting speed and feed rate of 240 m/min and 0.15 mm/rev, respectively. In these figures, the chip formation for low and high cutting speed can be observed. The first one is closer to the form of a continuous chip as the saw-teeth, areas of shear localization, are smaller and the distance between them is wide. In the second case, the saw-teeth of the chip are clearer visible and closer to one another. Bending of the chip is also more obvious. In the same figures, the temperature distribution in the workpiece, chip and cutting tool can also be observed. The temperatures for higher cutting speed are significantly higher; this observation concurs with the mechanism of the serrated chip formation presented earlier in this paper.

Higher temperatures in the cutting tool tip and the tool-chip interface coincide with the areas where tool wear is observed. Simulations may offer an insight into the mechanism of tool wear and consequently tool life.

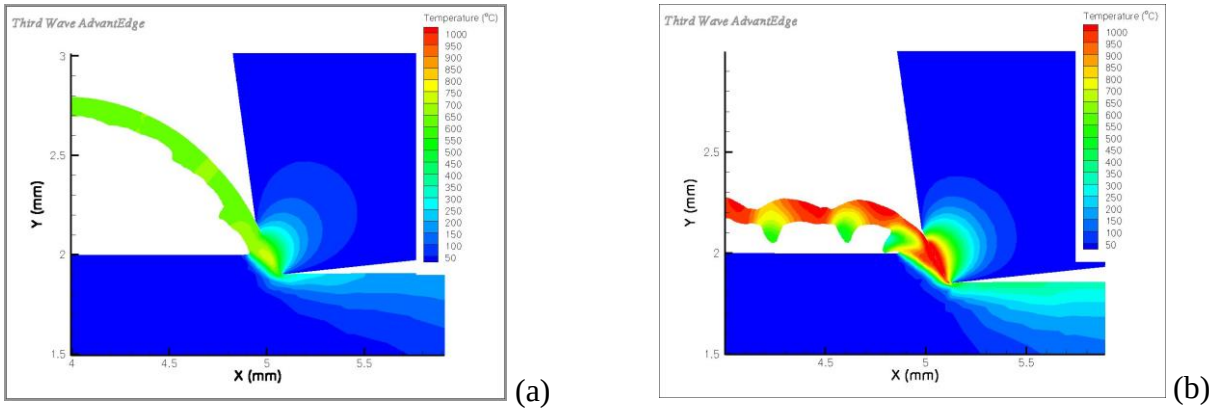

Figure 4: Temperature contours in the cutting zone for cutting speed and feed rate (a) 90 m/min; 0.10 mm/rev and (b) 240 m/min; 0.15 mm/rev.

Summary

In this paper the turning of 16MnCr5 steel with PCBN cutting tools is investigated. The investigation focuses on the analysis of the influence of cutting speed and feed rate on the components of the cutting force. For this purpose, experiments were conducted with various speeds and feed rates within the spectrum of the cutting conditions usually applied in industrial practice.

The results suggest the trends that cutting forces follow with increase in cutting speed and feed rate. An increase in cutting speed results in a decline to F_p, attributed to the elevation of the temperature in the cutting zone. It is observed that feed rate increase, increases F_p and F_c force components. However, for lower values of the cutting conditions F_p is much higher than F_c, resulting in high F_p/F_c ratio values, as a result of the feed being almost equal to the cutting edge radius of the cutting tool.

With the results of the experimental procedure, FEM models are constructed. The validity of the models is tested against the F_p and F_c force components, as the analysis pertains to 2D simulations, and the chip formation mechanism. The results of the FEM analysis follow closely the trends indicated by the experiments and also predict with accuracy the formation of the serrated chip; this type of chip is usual for this kind of machining and is reported in similar studies. Furthermore, the models are in position of providing numerical results on parameters of the process that are difficult to be obtained otherwise, e.g. elastic strain and temperature contours of the workpiece-chip-tool system. These results offer an insight on the conditions in the cutting zone and are in agreement with the theory of serrated chip formation. The models can be used for alternative cutting condition simulations for the prediction of critical parameters of the manufacturing process.

Acknowledgement

This research was partially carried out in the framework of the Center of Excellence of Innovative Engineering Design and Technologies at the University of Miskolc.

Furthermore the authors greatly appreciate the financial support of the National Research, Development and Innovation Office – NKFIH (No. of Agreement: OTKA K 116876).

References

[1] F. Klocke, G. Eisenblätter, Dry cutting, Annals of the CIRP 46(2) (1997) 519–526.

[2] J. Kundrák, A.G. Mamalis, A. Markopoulos, Finishing of hardened boreholes: grinding or hard cutting?, Materials and Manufacturing Processes 19(6) (2004) 979–993.

[3] G. Bartarya, S.K. Choudhury, State of the art in hard turning, International Journal of Machine Tools and Manufacture 53 (2012) 1–14.

[4] H. Ernst, H.B. Knowlton, J.W. Bolton, A.H. D' Arcambal, W.E. Bancroft, H.P. Croft, Machining of metals, ASM, Cleveland, OH, 1938.

[5] E.M. Trent, P.K. Wright, Metal cutting, Butterworth-Heinemann, Woburn, USA, 2000.

[6] G. Liyao,W. Minjie, D. Chunzheng, On adiabatic shear localized fracture during serrated chip evolution in high speed machining of hardened AISI 1045 steel, International Journal of Mechanical Sciences 75 (2013) 288–298.

[7] G.G. Yea, Y. Chen, S.F. Xue, L.H. Dai, Critical cutting speed for onset of serrated chip flow in high speed machining, International Journal of Machine Tools and Manufacture 86 (2014) 18–33.

[8] M. Bäker, Finite element simulation of high-speed cutting forces, Journal of Materials Processing Technology 176 (2006) 117-126.

[9] D.W. Tang, C.Y. Wang, Y.N. Hu, Y.X. Song, Finite-element simulation of conventional and high-speed peripheral milling of hardened mold steel, Metallurgical and Materials Transactions A 40A (2009) 3245-3257.

[10] H.M. Lin, Y.S. Liao, C.C. Wei, Wear behavior in turning high hardness alloy steel by CBN tool, Wear 264 (2008) 679–684.

[11] Y. Yang, and J.F. Li, Study on mechanism of chip formation during high-speed milling of alloy cast iron, International Journal of Advanced Manufacturing Technology 46 (2010) 43–50.

[12] G.M. Robinson, M.J. Jackson, A review of micro and nanomachining from a materials perspective, Journal of Materials Processing Technology 167 (2005) 316-337.

[13] G.R. Johnson, W.H. Cook, A Constitutive Model and Data for Metals Subjected to Large Strains, High Strain Rates and High Temperatures, in: Proceedings of the 7th International Symposium on Ballistics, The Hague, The Netherlands (1983) 541-547.

[14] Third Wave AdvantEdgeTM User's Manual, Version 5.1.

[15] W.S. Lee, C.F. Lin, High-Temperature Deformation Behavior of Ti6Al4V Alloy Evaluated by High Strain-Rate Compression Tests, Journal of Material Processing Technology 75 (1998) 127-136.

[16] S.P.F.C. Jaspers, J.H Dautzenberg, Material Behaviour in Conditions Similar to Metal Cutting: Flow Stress in the Primary Shear Zone, Journal of Material Processing Technology 122 (2002) 322-330.

[17] T. Özel, Y. Karpat, Identification of Constitutive Material Model Parameters for High-Strain Rate Metal Cutting Conditions Using Evolutionary Computational Algorithms, Materials and Manufacturing Processes 22 (2007) 659-667.

[18] J.P. Davim, C. Maranhão, A study of plastic strain and plastic strain rate in machining steel AISI 1045 using FEM analysis, Materials and Design 30 (2009) 160-165.

[19] ČSN 41 4220/ISO 683/11-70

[20] T.H.C. Childs, R. Rahmad, The effect of a yield drop on chip formation of soft carbon steels, Machining Science and Technology 13 (2009) 471-487.